Rheo-NMR of Semidilute Polyacrylamide in Water

P. T. Callaghan*,† and A. M. Gil‡

Institute of Fundamental Sciences-Physics, Massey University, Palmerston North, New Zealand, and Department of Chemistry, University of Aveiro, 3810-193 Aveiro, Portugal

Received October 28, 1999

ABSTRACT: Rheo-NMR ^{1}H spectroscopy has been performed on semidilute solutions of polyacrylamide (PAA) in water using a cylindrical Couette cell in which the solution in the annulus may be imaged in order to investigate spatially dependent NMR parameters. A number of interesting properties emerge. Shear banded flow is observed, in contrast to rheo-NMR studies of other semidilute polymers in which simple power-law shear thinning is found. Furthermore, we find that the PAA chain protons exhibit a marked T_2 reduction under shear and that the recovery on shear cessation is indicative of slow reorganizational dynamics. The observed T_2 recovery is multiexponential, the fast molecular relaxation times correlate well with the terminal times measured from the steady-state flow curve, and we interpret our findings in terms of shear-induced deformation of the Doi−Edwards tube. We suggest that slower relaxation processes may be due to hydrogen bond formation.

Introduction

Applications of nuclear magnetic resonance (NMR) methods in rheological studies on complex fluids can be broadly subdivided into two categories.[1] These are the use of NMR velocimetry to examine flow profiles in the various shear geometries in order to gain direct information regarding the flow curve and hence probe the nonlinear, shear-dependent viscosity[2] and the use of NMR spectroscopic techniques in order to gain insight regarding molecular order and dynamics under shear.[3] Both approaches have been used successfully in recent years, and in a sense, the power of "rheo-NMR" methodology is in the potential amalgamation of these two perspectives.[1]

Semidilute polymer solutions studied using rheo-NMR include monodisperse polystyrene in cyclohexane, in the vicinity of a demixing transition,[4] polydisperse poly(ethylene oxide) in water,[5] and Xanthan gum in water,[6,7] all of which where sheared in a concentric cylinder Couette cell. These studies indicated shear thinning in which the flow curve constitutive behavior could be well represented by a power law model[8,9] (viscosity $\eta \sim \dot{\gamma}^{n-1}$ where $\dot{\gamma}$ is the shear strain rate and n is the power law exponent) with values of n below unity. In the case of polystyrene below the demixing temperature, wall slip was observed.[4] Velocimetry measurements for the poly(ethylene oxide) system have also been made for tube flow,[2] and in that study additional measurements of polymer self-diffusion coefficients indicated a strong enhancement in diffusion above a critical shear rate, an effect which was interpreted as arising from a breakdown of polymer entanglements. In all of these velocimetry studies of semidilute polymer solutions, a monotonic variation in shear rate was observed with increasing stress across the shearing cell gap. Furthermore, when semidilute polystyrene solutions were studied in a cone-and-plate cell, for which the stress is quite uniform, a correspondingly uniform shear rate was found across the gap, a result which is quite consistent with monotonic flow curve properties.

By contrast, a very unusual behavior was observed in the system polyacrylamide/water. A 3% solution of very high ($>10^7$ Da) molecular weight polyacrylamide exhibited shear-banded flow when deformed in the gap of a cone-and-plate cell.[10] Shear banding is believed to arise from the existence of an unstable branch in the flow curve[11] and is an effect normally associated with highly monodisperse polymers,[12] in particular the class of amphiphilic wormlike micellar solutions for which the dissociation−recombination reaction motionally averages chain length polydispersity effects.[13−15] As a consequence, the existence of shear banded flow in semidilute solutions of polydisperse polyacrylamide in water is surprising indeed.

In the present paper we examine this polymer system in greater detail, in particular focusing on the combined use of NMR velocimetry and NMR spectroscopy, with the aim of examining molecular dynamics under shearing flow. The particular spectroscopic tool employed has been the use of proton T_2 relaxometry. We will show here that these relaxation times are particularly sensitive to shear, that in steady state they differentiate regions of banded flow, and that their transient response mirrors the terminal relaxation transients measured in mechanical measurements on the same polymer system.

We shall argue here that the T_2 effect that we measure is associated with chain alignment phenomena. In many respects the best NMR tool for investigating orientational ordering is that of deuterium NMR for which the electric quadrupole interaction provides a well-defined a localized probe whose NMR spectrum transforms under rotation as[16] $^1/_2(3\cos^2\theta - 1)$. Several rheo-NMR studies in which the deuteron−quadrupole interaction has been used as a measure of orientation and orientational order have been reported in recent years.[17−21] The disadvantage with deuterium NMR is the need to isotopically label the material and the low signal-to-noise ratios experienced with this particular nucleus. In the case of proton NMR, the through-space proton dipolar interaction plays a similar role in the quadrupolar interaction in the case of the deuteron. Consequently, where order exists, the protons should experience a residual, static dipolar interaction, although this interaction may be very weak in the case

† Massey University.
‡ University of Aveiro.

10.1021/ma9918203 CCC: $19.00
Published on Web 05/10/2000

of semidilute solutions where rapid segmental dynamics will motionally average the dipolar couplings. However, as will be apparent in the present study, the effects of chain alignment may have a significant influence on proton spin−spin (T_2) relaxation. For that reason we briefly summarize the important features of T_2 relaxation relevant to the work presented here.

T_2 (spin−spin) relaxation results in a loss of phase coherence and a decay of the NMR signal. The rate of relaxation is sensitive to the magnitude of the various spin interactions and also to their rate of fluctuation. The two key parameters which govern the rate are the average mean-squared strength of dipolar interaction, $\overline{\langle H_D^2 \rangle}$, and the correlation time, τ_c, for fluctuations of this interaction under the influence of molecular reorientation motion, where H_D is a dipolar Hamiltonian operator, $\langle ... \rangle$ represents a quantum expectation value, and the bar represents an ensemble average for the spin system of interest.[16] Note that we shall be concerned with the regime in which "motional narrowing" occurs, namely where $\overline{\langle H_D^2 \rangle}\tau_c^2 \ll 1$. Since the dipolar coupling strength for nearby protons in a typical polymer is on the order of 100 kHz, a reorientational fluctuation with correlation times shorter than a few microseconds will suffice.[22,23] While terminal relaxation times for high polymers may be much longer than this, the high degree of segmental mobility will generally result in rapid and nearly isotropic motional averaging.[22−24] In this regime, the spin−spin relaxation can be simply described by the relationship[16]

$$\frac{1}{T_2} \approx \overline{\langle H_D^2 \rangle}\tau_c \qquad (1)$$

$\langle H_D^2 \rangle$ is determined by a sum of local "through-space proton" dipolar interactions and hence varies as $\sum_{i,j} r_{ij}^{-6}$, where r_{ij} is an interproton distance. Whereas fluctuations in the dipolar interaction influence the T_2 relaxation, the time-averaged interaction strength $\Delta\omega_D \sim \overline{\langle H_D \rangle}$ may produce a spectral splitting or (static) dipolar broadening. Such static spectral broadening may be distinguished from relaxation broadening by means of specialized NMR echo experiments.[25,26] Under conditions of molecular deformation which will result from shearing or extensional flows, the parameters $\overline{\langle H_D \rangle}$, $\overline{\langle H_D^2 \rangle}$, and τ_c are all likely to be perturbed. Consequently, one might expect, in principle, to observe the influence of changes in molecular order and dynamics via both the static dipolar broadening and the change in T_2 relaxation.

Experimental Section

The polyacrylamide used in this work was a copolymer of acrylamide and the sodium salt of acrylic acid with respective monomer proportions of 60 and 40%. (Polysciences #464603, Warrington, PA). The nominal molecular weight was $>10^7$ Da, and the material was highly polydisperse (our estimate from GPC measurements is $M_w/M_n \approx 2.5$). PAA solutions were prepared using both H_2O and D_2O solvents with a range of polymer concentrations from 3.0 to 10.0% w/v. Proton NMR experiments were performed at 300 MHz and at a temperature of 25 C, using a Bruker AMX300 spectrometer equipped with microimaging attachment. The details of the velocity encoding method used in our work have been given elsewhere.[27] Using magnetic field gradient pulses, we encode the NMR signal both for nuclear spin position (**k**-encoding) and translational displacement (**q**-encoding over a fixed pulsed gradient spin-echo time interval, on the order of 20 ms.) The signal is acquired in two dimensions of **k**-space and one dimension of **q**-space, and a typical $128^2 \times 16$ data set takes on the order of 30 min using two signal-averaging steps. The data are Fourier analyzed in **q**-space in order to directly compute the local velocity distribution for each pixel of the spatially resolved image, allowing velocity resolution on the order of 10 mm s^{-1} at a spatial resolution of around $(20\ \mu m)^2$.

The rheo-NMR cell used in this work is shown in Figure 1. It consists of two concentric glass cylinders of outer diameter 9.4 mm and inner 7.4 mm, in which the inner cylinder rotates while the outer remains fixed. The cell is placed in the rf resonator of the NMR probe, and the inner cylinder is connected via a simple bayonet coupling to a drive shaft placed in central bore of the 7 T superconducting magnet and driven by a stepper motor and gearbox placed above the magnet. The drive unit is controlled by the NMR pulse program software on the spectrometer. The software is capable of turning the drive motor on and off in a predetermined manner, so that it is possible to acquire NMR spectra both during deformation and for successive periods of time following the cessation of deformation.

Independent mechanical measurements were performed using a Rheometrics RS500 stress-controlled rheometer, at a sample temperature of 25 °C.

Results

NMR Velocimetry of Semidilute Polyacrylamide/Water. NMR velocimetry measurements were carried out for a range of shear rates in the 3% solutions using both D_2O and H_2O solvents. In the H_2O solvent velocimetry measurements, solution was also placed in the inner rotating cylinder so that this unsheared material could provide a marker for the rigid body motion, thus enabling us to determine whether slip occurred at the inner wall. A selective excitation scheme was used[4] which enabled an image to be obtained in a selected region of the Couette cell, as shown in Figure 1b, for the 3% solution of PAA in H_2O. Notice the elliptical distortion of the image due to the use of a larger gradient in the direction normal to (i.e., across) the gap, the use of which enabled greater spatial resolution in this direction. Also shown in Figure 1 is a schematic diagram illustrating the associated regions of the annulus (sheared) fluid and marker (unsheared) fluid.

Figure 2 shows velocity profiles obtained for the solutions in H_2O solvent, at rotation speeds of 0.335**,** 0.509, and 0.684 Hz. No slip is apparent at either wall, but the solution exhibits heterogeneous shear, with a three-band structure obvious at the higher shear rates. Close to the inner wall there exists a region of low shear, further out is a high shear rate band, and then in the remaining region of the gap out to the outer wall a low shear rate band exists. Such three-band structure is reminiscent of that seen in a cylindrical Couette cell and cone-and-plate cell measurements on wormlike micelles.[28,29] We have also carried out velocimetry measurements for the 3% solution of PAA in D_2O at a rotation speed of 0.5 Hz. Because of the lower signal-to-noise ratio, few points were obtained across the gap; however, as apparent in Figure 2, the band structure observed is broadly similar to that found in the protonated solution.

***T_2* Relaxation Measurements in Steady State.** To investigate the effect of shear on T_2, we have carried out measurements in which a standard spin-echo sequence was used to weight the NMR signal by the factor $\exp(-2\tau/T_2)$ where τ is the delay time between the 90_x and 180_y rf pulses. Two classes of experiment were

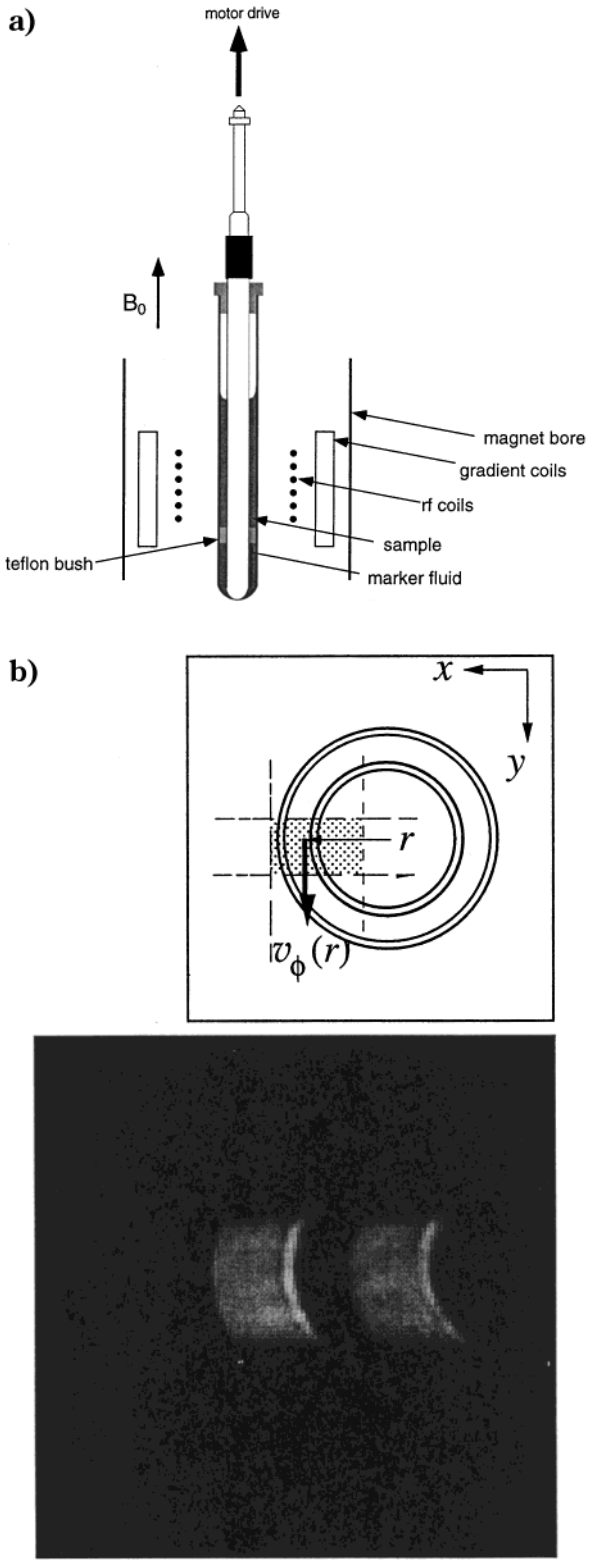

Figure 1. (a) Schematic diagram of cylindrical Couette cell used in this work. The fluid is sheared between glass inner and outer cylinders of 3.7 mm (o.d.) and 4.7 mm (i.d.), respectively. (b) Schematic cross section of the cell showing the region selected for imaging along with a sample NMR image obtained of fluid both in the annular gap and in the central cylinder. This latter fluid rotates as a rigid body and is used as a marker for the inner cylinder wall velocity.

performed, one in which the T_2 values were spatially resolved and the other in which they were spectrally resolved. We begin by presenting data for the spectrally resolved experiments where no imaging was performed.

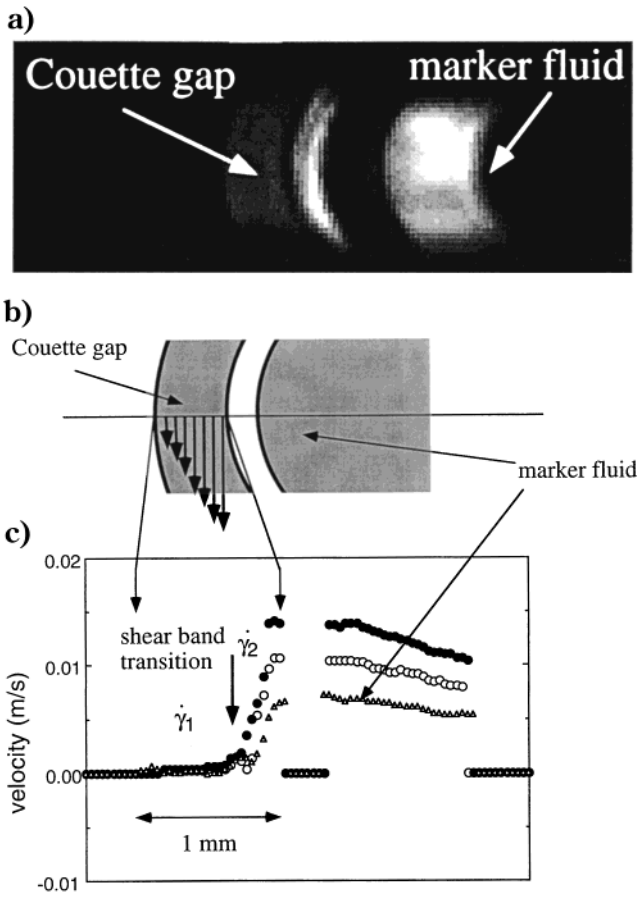

Figure 2. NMR velocimetry of 3% polyacrylamide in H_2O. (a) NMR intensity image from the 3.7 mm/4.7 mm Couette cell. The brighter band in the higher shear region is due to the higher velocity and fresh, fully relaxed, spins entering the image slice. (b) Schematic illustration of the cell geometry. (c) Velocity profiles for inner cylinder rotation speeds of 0.335 (diamond), 0.509 (open circles), and 0.684 Hz (closed circles).

For these experiments no solution was placed in the inner cylinder so that all signals arose from sheared annular fluid, albeit across different bands. The effect of shearing at 0.92 Hz is immediately apparent in the NMR spectra obtained using a spin echo with a fixed delay time of $2\tau = 10$ ms (i.e., the spectra are weighted by $\exp(-0.01/T_2)$ where T_2 is in seconds). A comparison of the ^{1}H NMR spectra (spectral width of 5 kHz) obtained with and without shear (inner cylinder rotation speed 0.92 Hz) is shown in Figure 3.

Figure 3a shows the ^{1}H NMR spectra obtained from 3% solutions of PAA in D_2O while Figure 3b shows the corresponding data for H_2O. The H_2O spectrum is dominated by the water peak, and even in D_2O, a significant water proton peak is apparent due to residual HDO. Clearly visible, in addition to the water protons, are peaks due to the amide NH_2 groups and the CH and CH_2 protons in the polymer chain. In D_2O it is clear that the amide protons have extensively exchanged with deuterons of the heavy water solvent, so that only a very small residual NHD signal is observable. The spectra shown in Figure 3 indicate a strong T_2 influence due to shearing for all protons on the polymer chain, but no effect for the protons of the water molecules.

To more closely examine the effect of shear, we have carried out spin-echo measurements over a range of echo times and analyzed the T_2 relaxation of all observable

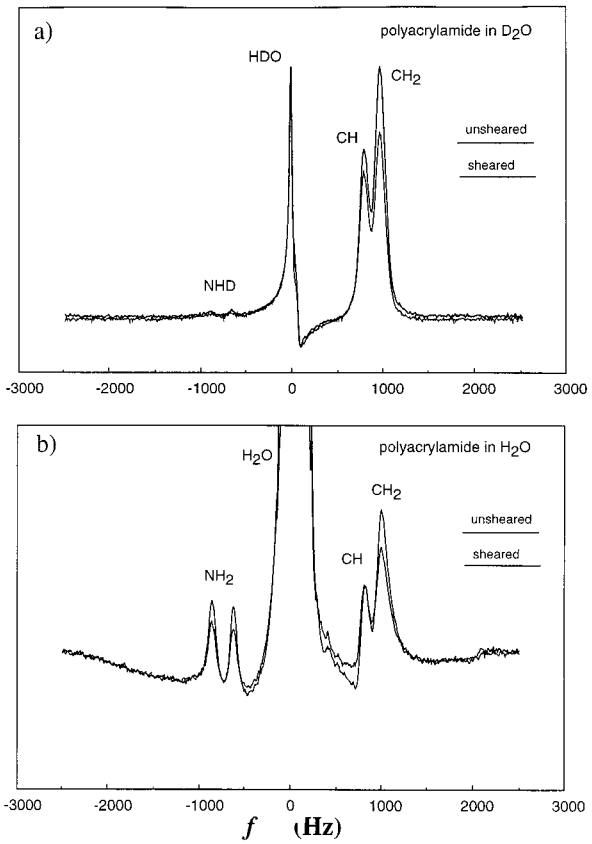

Figure 3. ^{1}H NMR spectra for 3% polyacrylamide in (a) D_2O and (b) H_2O under equilibrium conditions (dashed line) and under a shear of 10 s^{-1} (solid line). Note that for the D_2O experiment the T_1 of the proton NMR peak from residual HDO is much longer than the repetition time between acquisitions, leading to a phase distortion. Note further the weak proton NMR peaks from residual NHD sites where proton exchange with the solvent deuterons is incomplete.

Table 1. T_2 Values for Different Peaks in the ^{1}H NMR Spectrum of Polyacrylamide in H_2O and D_2O with and without Shearing (20 s^{-1})[a]

peak	T_2 (0 s^{-1}), ms	T_2 (20 s^{-1}), ms
	(a) Polyacrylamide in H_2O	
CH_2	13	9.5
CH	18	16
NH_2 (1)	23	19
NH_2 (2)	29	22
	(b) Polyacrylamide in D_2O	
CH_2	13	9.7
CH	17	13
NHD	120 ± 50	80 ± 50

[a] The accuracy is to the nearest significant figure quoted, except for the NHD protons in the polyacrylamide in D_2O sample where the error is much larger, as stated.

protons. The results are shown in Figure 4a,b, and the calculated T_2 values for all peaks are given in Table 1. In both the H_2O and D_2O solutions, the protons on the PAA exhibited a marked reduction in T_2 on shearing. Note the much longer relaxation times of the amide protons in the case of the D_2O solution. The weak signal from these resonances corresponds to NHD sites where the majority of protons have exchanged with deuterons from the water molecules, leaving an isolated proton whose weak dipolar interactions arise from distant proton sites. Finally, we note that no perceptible change in the H_2O or HDO T_2 values was found, indicating that the changes seen for the polymer protons were not due to an instrumental artifact caused by the fluid motion.

The spatially resolved T_2 experiment on PAA/D_2O involved varying the echo time, TE, in the rf/gradient pulse sequence used for spin warp encoding. As a result, all pixels in the image have a weighting $\exp(-TE/T_2)$. The range of intensities for different TE values is then analyzed via a nonlinear regression for each pixel to produce a T_2 value as well as the extrapolated intensity at zero echo time. While we note that echo time variation in a spin warp sequence can produce an additional contrast due to molecular self-diffusion, this effect is only important when the distance diffused by a molecule over the echo time becomes comparable with the pixel size. In the present experiment the polymer diffusion distance over the echo time is on the order of 0.1 μm, more than 2 orders of magnitude too small to have an effect.

The T_2 profile from the polymer proton signal (an average calculated for the dominant CH_2 and CH peaks) is shown in Figure 5, along with the corresponding velocity profile. It is clear that the average T_2 exhibits a distinct reduction in the sheared fluid with the most dramatic reduction apparent in the high shear band.

We will argue that the source of the T_2 change could be the reduction in configurational entropy and motional freedom associated with the deformation of the entanglement tube under shear. To establish this point, we describe now some experiments carried out under transient conditions in which the T_2 recovery is observed following cessation of shear. However, before leaving the spin echo contrast image data we note that it is possible to calculate, in addition, the extrapolated initial intensity image for the polymer protons. A corresponding profile is shown in Figure 5, and the results suggest, most remarkably, that there is an accretion of polymer in the high shear band region. It could be argued that concentration effects alone may be partly responsible for observed T_2 changes, but we will show in fact that the transient recovery of these changes on shear cessation correlates nicely with relaxation of polymer deformation.

***T_2* Relaxation in Transient Flow.** To ascertain the origin of T_2 relaxation enhancement, we have carried out a series of experiments in which the semidilute solution was sheared for a period and then suddenly stepped to zero shear, during which the proton T_2 values are continuously monitored by observing the intensity of each peak in the proton NMR spectrum obtained using a spin-echo pulse sequence in which the echo delay was fixed at $2\tau = 10$ ms. The use of such a sequence results in a relaxation contrast of the form $\exp(-2\tau/T_2)$. Notice that the data shown in Figure 4 suggest that the proton T_2 relaxation process is single-exponential. As we shall subsequently show, the much slower time evolution of proton T_2 values due to polymer terminal relaxation is multiexponential. We emphasize the difference between these different relaxation processes by noting their very different time scales, spin-relaxation times being on a millisecond scale and polymer terminal relaxation on a scale of many seconds.

In Figure 6a we show the result of an experiment on the 10% PAA/D_2O solution in which that sample is sheared at 10 s^{-1} for a few minutes and then the motor is switched off. The data exhibit distinct intensity changes in the CH/CH_2 region of the spectrum, although none at the water proton resonance. The slow recovery of the signal following shear cessation has a time

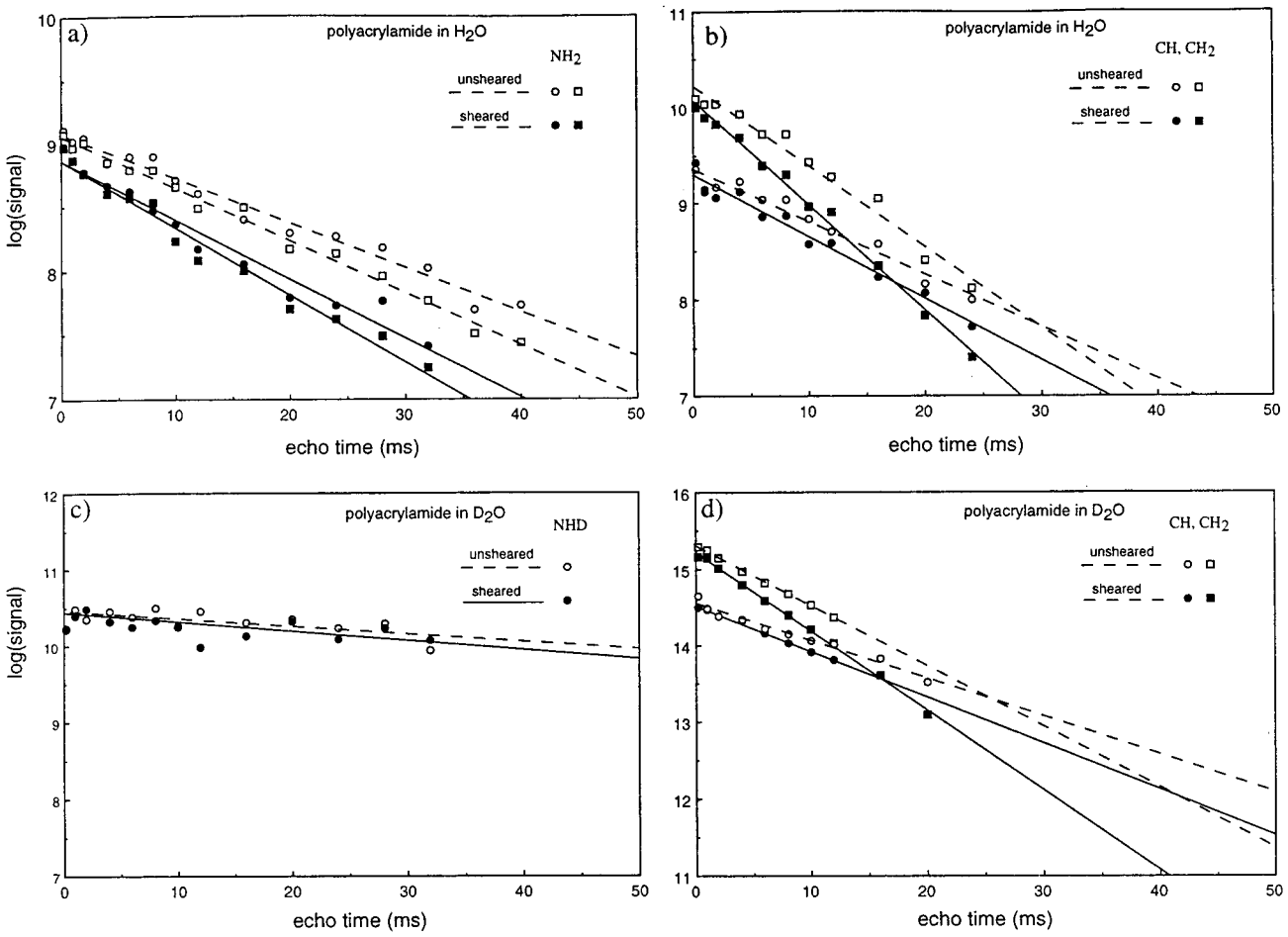

Figure 4. Log(signal) vs echo time for the proton NMR peaks indicated in Figure 3 for (a, b) 3% polyacrylamide in H_2O and (c, d) 3% polyacrylamide in D_2O, where open symbols correspond to measurements taken in equilibrium while the closed symbols are for shearing at 20 s^{-1}. Note that the scatter in the data is too large to accurately ascertain relaxation times for the very slowly relaxing HDO protons in (c).

constant on the order of 10 s. We shall show that this is comparable with the terminal relaxation time observed in the nonlinear rheology.

We have made measurements of the T_2 recovery process in a set of solutions at concentrations of 3%, 4%, 5%, 6%, 8%, and 10% w/v, in both D_2O and H_2O. Figure 6b shows the data for the 3% PAA/D_2O solution, while Figure 6c shows an equivalent transient behavior for 3% PAA/H_2O. The time evolution of the CH/CH_2 signal intensity in the H_2O samples was much more difficult to measure due to dynamic range problems associated with the large adjacent water peak and the strong influence on the CH/CH_2 signal intensity due to small phase changes in the dominant water signal. Each spectrum needed to be individually phased, and Figure 6c shows the selection used to ascertain the transient recovery.

The T_2 transients may be compared with characteristic viscometric relaxation times for the same set of solutions. We have measured the steady-state flow curve for each of these solutions in order to obtain the polymer terminal relaxation time from the onset of shear thinning. The curves for 3% and 10% are shown in Figure 7. By fitting the flow curves, using the Doi−Edwards model[30] for the constitutive behavior of entangled (monodisperse) polymers, the effective tube disengagement time, τ_d, was estimated. The dependence of τ_d on concentration is shown in Figure 8. We note that the concentration dependence is weaker than the reptation prediction (c^{-3}), an effect which we attribute to the high degree of chain-length polydispersity.

To compare the time constants for T_2 recovery with those found in the rheometric flow curve measurements, we have analyzed the spin-echo intensity data, for which the weighting is $\exp(-2\tau/T_2)$, by taking the log of the intensity to yield T_2^{-1} vs time data. Then we plot log T_2^{-1} vs time in order to obtain the appropriate time constants in the decay of T_2^{-1}. The resulting decay curves are shown in Figure 9. Note the much better signal-to-noise ratios obtained using the D_2O solvent. In the case of the H_2O solvent the large water peak limited the receiver gain and the dynamic range, thus creating a signal-to-noise degradation in the analysis of the weaker CH_2/CH resonances.

In the case of the D_2O solution data, where the signal-to-noise ratio of the polymer proton resonances was sufficiently good to follow the decay over more than a decade, the data clearly indicated more than one time constant. We have analyzed these decays using a regularized nonnegative least-squares (NNLS) routine[31] to provide an inverse Laplace transform. Examples of the relaxation spectra for 3% and 10% PAA/D_2O solutions are shown in Figure 10. In each case a slow time constant in the range 50−200 s was observed, along with a shorter time constant of between 7 and 20 s. We are not able to offer a clear explanation for the presence of these two time constants, although we would suggest that one is closely linked to the tube disengagement

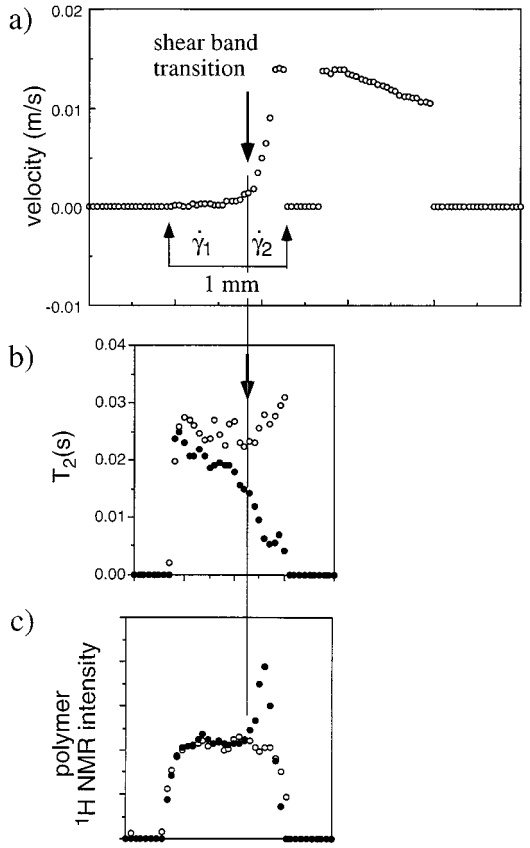

Figure 5. T_2 and ^{1}H NMR signal intensities as a function of radial position across the Couette cell annulus. (a) shows the velocity profile obtained at 0.68 Hz, as shown in Figure 2. In (b) and (c) are the T_2 and intensity profiles, respectively, with open circles being for zero shear and closed circles for an inner cell rotation speed of 0.5 Hz. The latter profile is obtained by extrapolating the spin-echo intensities in each pixel to zero echo time. Note the T_2 reduction which is most obvious in the vicinity of the shear band. A large increase in apparent polymer polymer concentration is observed in the high shear rate band.

process. The physical basis for this suggestion is discussed in the next section. For the moment we compare, in Figure 8, the mechanically measured disengagement times with the fast time constants found in the T_2 recovery data. We note with interest that the NMR-measured and mechanically measured time constants scale in the same way with concentration, albeit with a consistently longer value found in the flow curve analysis.

Discussion

The observation that shearing deformation induces proton NMR T_2 relaxation time changes for polymers in semidilute solution is, to our understanding, a novel result. In attempting to understand the source of these changes and their significance in the study of polymer solution rheology, we focus our attention on the following results. First, the relaxation rate changes occur for all protons on the polymer chain, although the magnitude of these changes varies somewhat. There is no perceptible change in the T_2 of the water protons. Second, the degree of change depends on local shear rate within the solution, a fact that is apparent in Figure 5 where the greatest reduction in average T_2 occurs in the vicinity of the high shear rate band. Finally, on cessation of shear, the transient properties of the T_2

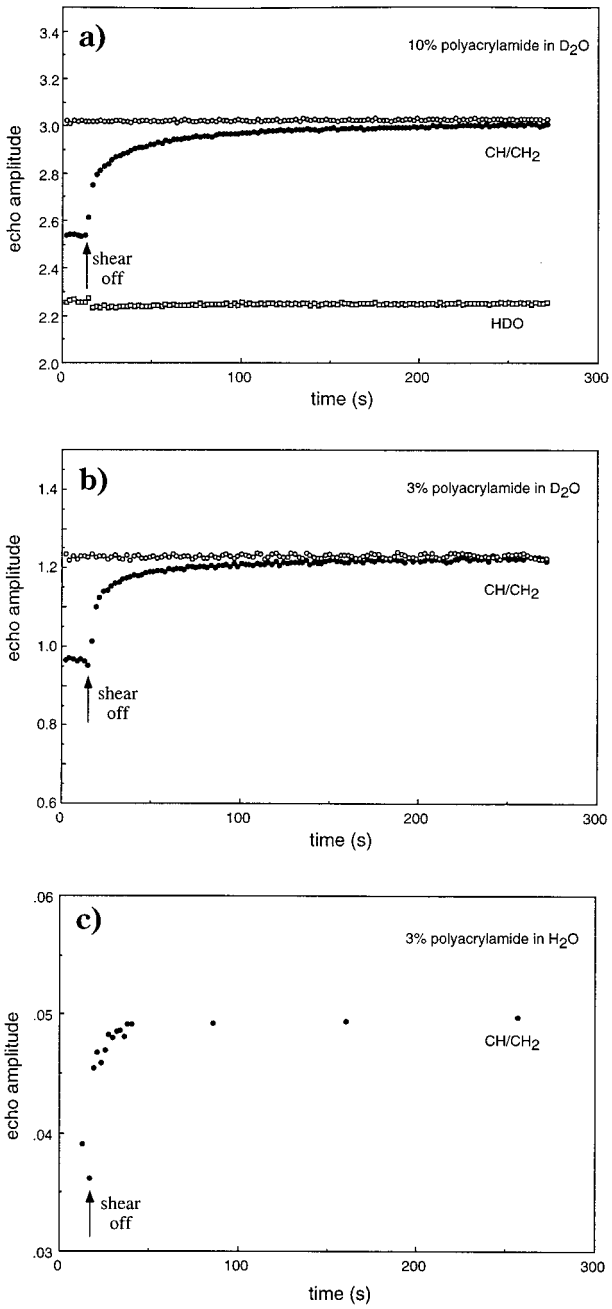

Figure 6. Recovery of the spin-echo signal obtained at a fixed delay $2\tau = 10$ ms for the CH/CH_2 region (solid circles) of the spectrum in (a) 10% polyacrylamide in D_2O, (b) 3% polyacrylamide in D_2O, and (c) 3% polyacrylamide in H_2O. In (a) and (b) the open circles show the equilibrium baseline echo intensity obtained some minutes later after full relaxation. In (a) the behavior of the water (HDO) peak is shown. This exhibits a much weaker, but observable, transient effect, probably due to baseline effects arising from neighboring polymer proton resonances.

recovery to equilibrium exhibit more than one exponential time constant, in the case of the better resolved D_2O data. The more rapid of these time constants was of a similar order of magnitude to the tube disengagement time as measured mechanically and exhibited a similar concentration dependence. These factors lead us to the conclusion that the T_2 changes are associated with conformational constraints closely connected with the Doi−Edwards tube and that reptation within the tube, leading to tube disengagement, is the source of relaxation of these conformational constraints.

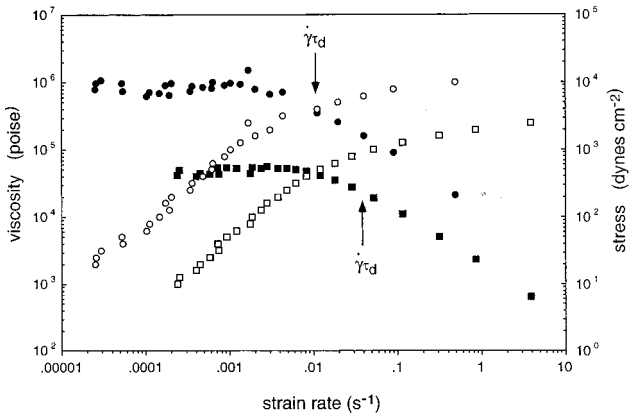

Figure 7. Flow curves (viscosity and stress vs shear rate) for 10% polyacrylamide in D_2O (circles) and 3% polyacrylamide in D_2O (squares) where the open symbols give the stress and the closed symbols the viscosity. The Deborah numbers corresponding to unity, based on the Doi−Edwards model, are shown in each case.

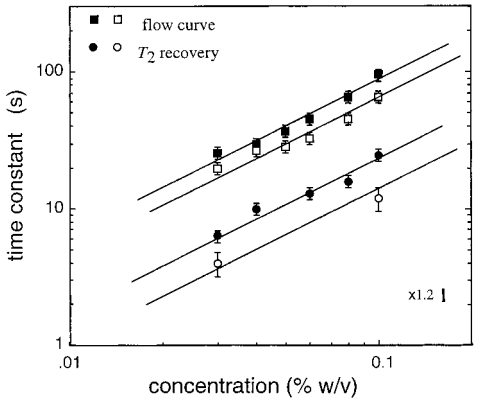

Figure 8. Terminal relaxation times, τ_d, obtained by Doi−Edwards analysis of the flow curves (squares), compared with polymer relaxation times (circles) obtained from the fast component decay of the proton T_2 values following cessation of shear. In each case the closed symbol is for the D_2O solution and the open symbol for the H_2O solution. The scaling lines shown correspond to an exponent of 1.2.

Our picture is as follows. For semidilute polymers the effect of surrounding chain entanglements is to produce a hierarchy in the motional averaging process. Rapid segmental motion will motionally average most of the dipolar interactions between neighboring protons, but the effect of the entanglement tube is to leave a residual degree of orientational order which can only be averaged to zero by the much slower one-dimensional curvilinear diffusion of the polymer along the primitive path of the tube. The preaveraged dipolar Hamiltonian, $H_D(t)$, results in a corresponding dipolar precession frequency, $\omega_D(t)$. The final motional averaging step thus occurs with a correlation time on the order of the time taken to diffuse around a tube bend. The effect of this hierarchy on T_2 relaxation is shown schematically in Figure 11.

In the model of Doi and Edwards,[30] the effect of shearing flow is to affinely deform the entanglement tube, and under strong shear this results in a significant extension along the velocity direction. Note that deformations of the tube and the individual polymer molecules are not identical. For shear rates in excess of the tube disengagement rate, τ_d^{-1}, but smaller than the Rouse rate τ_R^{-1} (the situation encountered here) the polymer retains its natural Rouse length, albeit distributed along the curvilinear tube path, but that path itself is deformed. Two consequences will emerge. First, there will exist a degree of orientational ordering of the tube, and this should result in a weak residual dipolar interaction being observed. Second, the curvilinear length around tube bends will increase, as indicated in Figure 11, leading to a slower correlation time for the final orientational motional averaging step and, hence, a faster T_2 relaxation rate.

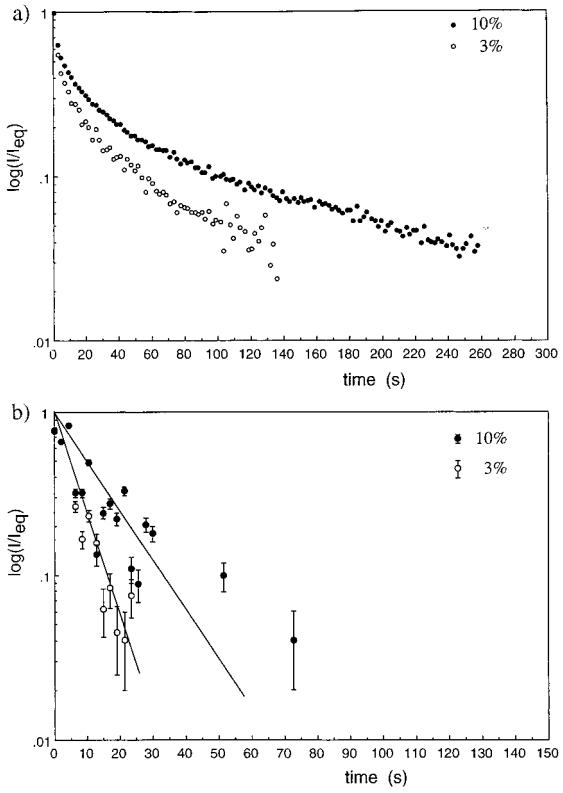

Figure 9. Decay following shear cessation of the log(echo amplitude) for (a) 3% and 10% polyacrylamide in D_2O and (b) 3% and 10% polyacrylamide in H_2O. Note the much poorer signal-to-noise ratios obtained in H_2O because of dynamic range problems associated with the strong water resonance. In (b) the straight lines correspond to decay times of 12 ± 2 and 5 ± 1 s for 10% and 3% solutions, respectively.

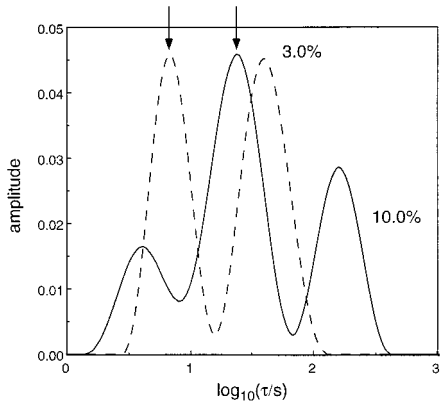

Figure 10. Nonnegative least-squares Laplace inversion of the 3% and 10% polyacrylamide in D_2O T_2 recovery on shear cessation data shown in Figure 9a. A multiexponential distribution is assumed, and the amplitude of each exponential is calculated over the chosen range of decay times, τ. The arrows indicate the fast relaxation mode in each case. The weak peak at short relaxation time for the 10% data is probably an artifact due to difficulty in precisely defining the time origin in the shear cessation experiment.

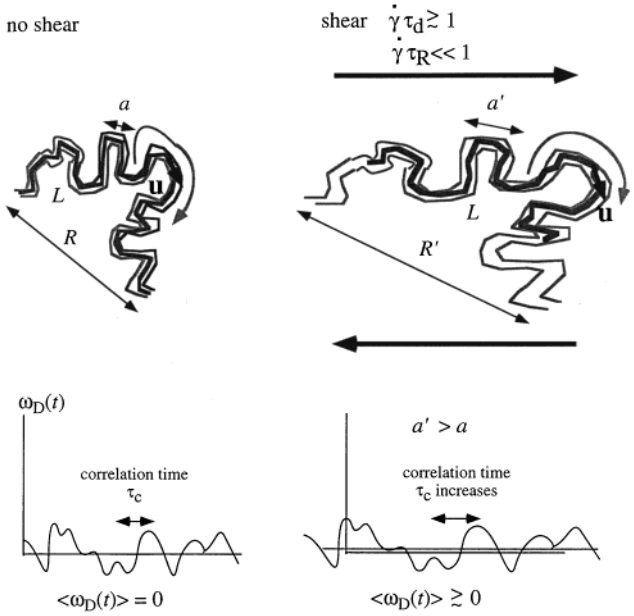

Figure 11. Schematic diagram illustrating the effect of shear in deforming the entanglement tube. We postulate that this leads to a greater correlation length for reorientation by curvilinear diffusion and a longer reorientational correlation time and shorter T_2.

The polymer terminal relaxation times, as indicated by the T_2 transient measurements, are nearly 1 order of magnitude shorter than those observed in the flow curve analysis. This may partly reflect the difficulties that can arise when comparing terminal times obtained under steady shear and transient shear conditions, especially for a polydisperse material. It may also reflect the very different nature of the detection process, in the one case by the relaxation of stress and in the other in the relaxation of the constraints to reorientation of the dipolar interaction. In may well be that the dipolar reorientation effect is more sensitive to higher order (i.e., faster) internal Rouse modes of the entanglement tube than to the final disengagement process.

It has been previously shown that strong shearing flows can produce weak static spectral broadening due to dipolar interactions in polymer melts.[21] We have attempted to measure such effects in the semidilute PAA solutions using the combined solid/Hahn echo ("beta") technique, which results in a sine-correlation function very sensitive to weak dipolar terms in the spin Hamiltonian. We are unable to measure any dipolar interaction in excess of a few hertz in strength, the lower limit of sensitivity of our method. We therefore conclude that the relatively higher segmental mobility of semidilute polymers, compared with that which exists in the molten state, makes such effects very difficult to observe. However, the increase in correlation time, τ_c, associated with tube deformation is clearly significant and, as indicated by eq 1, is able to lead to the T_2 change which we have observed in our work.

If such a model is correct, then the recovery of T_2 on shear cessation is explained. Tube disengagement enables the deformed entanglement field to relax back to its equilibrium isotropic state, so that the proton T_2 value closely tracks this process. The origin of the much slower time constant seen in Figure 10 is interesting, and while we cannot be certain of its cause, we are inclined to speculate that it arises from intermolecular interactions, possibly associated with the formation of hydrogen bonds established between neighboring amide groups. Evidence that hydrogen bonding may important can be found in the terminal relaxation time data shown in Figure 8. If the viscosity of the solvent were the only factor determining the reptational dynamics in D_2O and H_2O solutions of identical polymer at the same concentration, then the ratio of disengagement times should be 1.2[32] as indicated by the bar in Figure 8. In fact, that ratio is around a factor of 2 greater. We do not believe that this difference arises from a difference in solvent quality and hence coil size, since the θ temperature is well below room temperature for this system so that deuteration should not significantly alter the status of water as a good solvent. Hence, we argue that additional intermolecular or solvent−molecular interactions are responsible for the apparent difference in chain friction. Furthermore, we would argue that semidilute polyacrylamide in water exhibits slow dynamical behavior which is not simply reptation-based, by virtue of the fact that significant shear banding is found in this system, yet not found at all for other semidilute solutions, even those for which the polymer distribution is very monodisperse. We suggest that the origin of shear banding in (relatively polydisperse) polyacrylamide solutions is associated with hydrogen bond breakage above a critical shear rate.

Finally, we draw attention to the enhanced concentration of polymer found in the vicinity of the high shear band. In shearing flow the free energy may be influenced by chain deformation so that the chemical potential of each molecule is not simply related to concentration as in the ideal gas. In the model of Olmsted and Lu,[33] the equality of the chemical potential between polymer in adjacent shear bands may be associated with a discontinuity ion polymer concentration. The rather large concentration differences apparent in our work may in part arise from an artifact of the extrapolation process used to analyze the relaxation decay in each image pixel. However, we note that such a large difference was not seen in other shear banded systems studied in our laboratory. Thus, we believe that they are real and may be a manifestation of strong free energy perturbations in the shear band structure.

Conclusion

The NMR velocimetry and spectroscopy data presented here indicate that semidilute polyacrylamide solutions in water exhibit heterogeneous flow in shear and that proton spin−spin relaxation rates are increased as a result of shearing flow, an effect which we attribute to entanglement tube deformation. The transient behavior of the relaxation times on cessation of shear is multiexponential, with the fast component correlating, in its concentration dependence, with the terminal relaxation time as measured from the flow curve. The slower transient behavior may be due to hydrogen-bonding effects.

T_2 relaxation is a particularly easy NMR parameter to measure and may be equally easily used as a contrast in spatially resolved experiments. Consequently, the use of T_2 perturbation as a probe of molecular conformational or organizational changes should prove a particularly useful tool in rheo-NMR studies of complex fluids, especially for those where changes occur sufficiently slowly that the T_2 change can be observed as a transient.

Acknowledgment. P.T.C. is grateful to the New Zealand Foundation for Research, Science and Technology and to the Royal Society of New Zealand for funding support under the Public Good Science Fund and the Marsden Fund. A.M.G. acknowledges the Foundation for Science and Technology in Portugal for partial funding through the project PRAXIS/PCNA/BIO/0703/96.

References and Notes

(1) Callaghan, P. T. *Rep. Prog. Phys.* **1999,** *62* , 599.
(2) Xia, Y.; Callaghan, P. T. *Macromolecules* **1991**, *24*, 4777.
(3) Nakatani, A. I.; Poliks, M. D.; Samulski, E. T. *Macromolecules* **1990,** *23*, 2686.
(4) Manz, B.; Callaghan, P. T. **1997**, *30*, 3309−3316.
(5) Rofe, C. J.; Lambert, R. K.; Callaghan, P. T. *J. Rheol.* **1994**, *38*, 875.
(6) Rofe, C. J.; de Vargas, L.; Pérez-González, J.; Lambert, R. K.; Callaghan, P. T. *J. Rheol.* **1996**, *40*, 1115.
(7) Gibbs S. J.; James, K. L.; Hall, L. D.; Haycock, D. E.; Frith, W. J.; Ablett, S. *J. Rheol.* **1996**, *40*, 425.
(8) Walters, K. *Rheometry;* Chapman and Hall: London, 1975.
(9) Skelland, A. H. P. *Non-Newtonian Flow and Heat Transfer*; Wiley: New York, 1967.
(10) Britton, M. M.; Callaghan, P. T. *J. Rheol.* **1997**, *41*, 1365.
(11) Cates, M. E.; McLeish, T. C. B.; Marrucci, G. *Europhys. Lett.* **1993**, *21*, 451.
(12) McLeish, T. C. B.; Ball, R. C. *J. Polym. Sci.* **1986**, *24* , 1735.
(13) Cates, M. E. *J. Phys. Chem.* **1990**, *94*, 371.
(14) Cates, M. E. *Macromolecules* **1987**, *20*, 2289.
(15) Spenley, N. A.; Cates, M. E.; McLeish, T. C. B. *Phys. Rev. Lett.* **1993**, *71*, 9.
(16) Abragam, A. *Principles of Nuclear Magnetism*; Oxford University Press: New York, 1963.
(17) Grabowski, D. A.; Schmidt, C. *Macromolecules* **1994**, *27*, 2632.
(18) Lukaschek, M.; Grabowski, D. A.; Schmidt, C. **1995**, *11*, 3590.
(19) Lukaschek, M.; Muller, S.; Hansenhindl, A.; Grabowski, D. A.; Schmidt, C. *Colloid Polym. Sci.* **1996**, *274*, 1.
(20) Siebert, H.; Grabowski, D. A.; Schmidt, C. *Rheol. Acta* **1997**, *36*, 618.
(21) Callaghan, P. T.; Kilfoil, M. L.; Samulski, E. T. *Phys. Rev. Lett.* **1998**, *81*, 4524.
(22) Cohen-Addad, J. P. *Prog. NMR Spectrosc.* **1993**, *25*, 68.
(23) Kimmich, R.; Schnur, G.;Kopf, F. M. *Prog. NMR Spectrosc.* **1988**, *20*, 385.
(24) Callaghan, P. T.; Samulski, E. T. *Macromolecules* **1998**, *31*, 3693.
(25) Kimmich, R. *NMR: Diffusometry, Relaxometry and Tomography*; Springer: Berlin, 1997.
(26) Callaghan, P. T.; Samulski, E. T. *Macromolecules* **1997**, *30*, 113.
(27) Callaghan, P. T. *Principles of NMR Microscopy;* Oxford University Press: Oxford. 1991.
(28) Mair, R. W.; Callaghan, P. T. *Europhys. Lett.* **1996**, *36*, 719.
(29) Britton, M. M.; Callaghan, P. T. *Phys. Rev. Lett.* **1997**, *78*, 4930.
(30) Doi, M.; Edwards, S. F. *The Theory of Polymer Dynamics*; Oxford University Press: Oxford, 1987.
(31) Lawson, C. L.; Hanson, R. J. *Solving Least Squares Problems*; Prentice-Hall: Englewood Cliffs, NJ. 1974.
(32) Vinogradov, S. N.; Linnell, R. H. *Hydrogen Bonding;* Van Nostrand Reinhold: New York, 1971.
(33) Olmsted. P. D.; Lu, C.-Y. D. *Phys. Rev. E* **1997**, *56*, R55.

MA9918203